Published online 28 November 2017

Nucleic Acids Research, 2018, Vol. 46, No. 2 ***689–703***
doi: 10.1093/nar/gkx1208

Acetylation of 53BP1 dictates the DNA double strand break repair pathway

Xiang Guo[1], Yongtai Bai[1], Meimei Zhao[1], Mei Zhou[1], Qinjian Shen[1], Cai-Hong Yun[2], Hongquan Zhang[3], Wei-Guo Zhu[4] and Jiadong Wang[1,*]

[1]Institute of Systems Biomedicine, Department of Radiation Medicine, School of Basic Medical Sciences, Peking University Health Science Center, Beijing 100191, China, [2]Department of Biophysics, Shenzhen University Health Science Center, Shenzhen 518060, China, [3]Department of Anatomy, Histology and Embryology, Shenzhen University Health Science Center, Shenzhen 518060, China and [4]Department of Biochemistry and Molecular Biology, Shenzhen University Health Science Center, Shenzhen 518060, China

Received September 18, 2017; Revised November 17, 2017; Editorial Decision November 20, 2017; Accepted November 22, 2017

ABSTRACT

P53-binding protein 1 (53BP1) plays critical roles in DNA double strand break (DSB) repair by promoting non-homologous end joining (NHEJ), and loss of 53BP1 abolishes PARPi sensitivity in BRCA1-deficient cells by restoring homologous recombination (HR). 53BP1 is one of the proteins initially recruited to sites of DSBs via recognition of H4K20me2 through the Tudor-UDR domain and H2AK15ub through the UDR motif. Although extensive studies have been conducted, it remains unclear how the post-translational modification of 53BP1 affects DSB repair pathway choice. Here, we identified 53BP1 as an acetylated protein and determined that acetylation of 53BP1 inhibit NHEJ and promote HR by negatively regulating 53BP1 recruitment to DSBs. Mechanistically, CBP-mediated acetylation of K1626/1628 in the UDR motif disrupted the interaction between 53BP1 and nucleosomes, subsequently blocking the recruitment of 53BP1 and its downstream factors PTIP and RIF1 to DSBs. Hyperacetylation of 53BP1, similar to depletion of 53BP1, restored PARPi resistance in BRCA1-deficient cells. Interestingly, 53BP1 acetylation was tightly regulated by HDAC2 to maintain balance between the HR and NHEJ pathways. Together, our results demonstrate that the acetylation status of 53BP1 plays a key role in its recruitment to DSBs and reveal how specific 53BP1 modification modulates the choice of DNA repair pathway.

INTRODUCTION

DNA double strand breaks (DSBs) are the most dangerous chromosomal lesions; they not only cause permanent cell cycle arrest and cell death but also induce cell transformation and tumorigenesis (1,2). The accurate repair of DSBs is crucial for maintaining genomic stability and preserving cellular homeostasis (3,4). Eukaryotic cells have two distinct DSB repair pathways, non-homologous end joining (NHEJ) and homologous recombination (HR) (3,4).

P53-binding protein 1 (53BP1) is an important factor for class switch recombination and a key regulator of DSB processing and repair by NHEJ (5,6). One of the most striking findings regarding 53BP1 is that its deficiency almost completely reverses the phenotype of BRCA1 deficiency, including in tumorigenesis, embryonic lethality and PARPi sensitivity (7–10). Recent studies have shown that 53BP1 dictates the DSB repair pathway by promoting NHEJ-mediated DSB repair while preventing DNA end resection-dependent HR (11,12). The decision of which pathway to utilize for DSB is tightly controlled by the cell cycle and is critical for avoiding inaccurate DNA repair and maintaining genomic stability (2,4,5).

Although 53BP1 lacks apparent enzymatic activity, it functions by cooperating with downstream factors in a phosphorylation-dependent or phosphorylation-independent manner (2,6). 53BP1 is a large protein that contains multiple interaction surfaces and structural elements, including BRCT and Tudor domains (2,6). 53BP1 is usually considered a mediator of DSB signaling because it recruits numerous DSB-responsive proteins, such as expand1, PTIP and RIF1 (11–19).

53BP1, similar to many other DNA damage response (DDR) and repair proteins, must accumulate at sites of DNA DSBs to accomplish its functions (2,6). 53BP1 is one of the proteins initially recruited to DSB sites via recognition of H4K20me2 through the Tudor-UDR do-

*To whom correspondence should be addressed. Tel: +86 10 82802450; Email: wangjiadong1980@hotmail.com

main and H2AK15ub through the UDR motif. This process is driven by a Tip60-ATM-mediated signaling cascade involving ATM-γ-H2AX-MDC1-RNF8/RNF168 and the activation of RNF8/RNF168-dependent chromatin ubiquitination (2,6,20–26). Moreover, RNF169 antagonizes the ubiquitin-dependent signaling cascade at DSBs and represses 53BP1 accumulation at DNA damage sites (27–30). Upon DNA damage, KDM4A/JMJD2A is degraded by RNF8/RNF168, leading to exposure of H4K20me2, which is critical for recognition by the tandem Tudor domain of 53BP1 (31). In addition, L3MBTL1 and TIRR repress the targeting of 53BP1 to DNA damage sites by masking the interaction between H4K20me2 and the Tudor domain of 53BP1 (32–35). Recent studies have also shown that the UDR domain of 53BP1 is essential for its recruitment to DNA damage sites by facilitating nucleosome binding through H2AK15 recognition, which is independent of Tudor domain-mediated H4K20me2 recognition (36–38). Further study revealed that the UDR of 53BP1 is a reader of the DNA-damage-induced H2A Lys 15 ubiquitin mark and also is required for 53BP1 foci formation (37,38). ATM-mediated phosphorylation of the N-terminus of 53BP1 directly recruits the downstream factors PTIP/Artemis and RIF1/Rev7 (39–41). 53BP1, PTIP and RIF1 form a stable complex to compete with BRCA1 and inhibit CtIP-mediated end resection in HR.

Post-translational modifications, including phosphorylation, ubiquitination, ADP-ribosylation and methylation, play critical roles in regulating DNA repair factors at ionizing radiation (IR)-induced foci (IRIF) and are essential for the repair of DNA DSBs (2,42,43). Phosphorylation of 53BP1 by ATM is required for the recruitment of the downstream factors PTIP and RIF1 (11–13,16,17). It also has been shown in the previous study that 53BP1 is phosphorylated during mitosis on two residues, T1609 and S1618, also located in its UDR motif (44,45). Phosphorylating these sites blocks the interaction of the UDR motif with nucleosomes containing ubiquitinated histone H2A and impedes binding of 53BP1 to mitotic chromatin (44,45). Misregulation of this modification renders telomeres fusion and mitotic defect (44,45). Moreover, UbcH7 or RNF168 is involved in regulating 53BP1 ubiquitination and regulating its protein stability or the initial recruitment of 53BP1 to DSBs, respectively (46,47). Although extensive study about the post-translational modifications of 53BP1, it still remains unclear whether other post-translational modifications are involved in regulating 53BP1 function. Because 53BP1 plays a central role in DSB repair by mediating NHEJ and in PARPi resistance in BRCA1-deficient cells by restoring HR, it is crucial to identify novel post-translational modifications of 53BP1 and to determine whether and how specific 53BP1 modification is important for DNA repair and drug resistance.

In this study, we identified 53BP1 as an acetylated protein and found that acetylation of 53BP1 negatively regulates its recruitment to DSBs. CBP-mediated acetylation of K1626/1628 in the UDR motif disrupted the interaction between 53BP1 and nucleosomes, subsequently blocking the recruitment of 53BP1 and its downstream factors PTIP and RIF1 to DSB sites. Hyperacetylation of 53BP1, similar to depletion of 53BP1, restored PARPi resistance in BRCA1-deficient cells. Interestingly, 53BP1 acetylation was tightly regulated by HDACs to maintain balance between the HR and NHEJ pathways. Together, our results demonstrate that the acetylation of 53BP1 plays a key role in its recruitment to DSBs and reveal how specific 53BP1 modification modulates the choice of DNA repair pathway.

MATERIALS AND METHODS

Cell culture and plasmids

HEK293T, HEK293A and HeLa cells were cultured in DMEM supplemented with 10% fetal bovine serum and 1% penicillin/streptomycin. All cells were incubated in a humidified ECSO incubator with 5% CO_2. All cDNAs were subcloned into pDONR201 (Invitrogen) as entry clones and subsequently transferred to gateway-compatible destination vectors for the expression of N- or C-tagged fusion proteins. All deletion mutants and point mutants were generated by PCR and verified by sequencing. HA-CBP, HA-CBP-Y1503F, HA-p300, Flag-Gcn5, Flag-Myst1 and Flag-Myst2 were gifts from Dr Jianyuan Luo.

Antibodies

The Ac-K1626/1628–53BP1 polyclonal antibody was generated and purified using the following peptide: aa 1620–1636, (C)DNLVEGK(Ac)RK(Ac)RRSNVSSP. The following specific antibodies were used: 53BP1 (612522, BD, San Jose, CA, USA), RPA32 p(S4/S8) (A300-245, Bethyl Laboratories), CBP (D6C6, Cell Signaling), HDAC2 (A0867, ABclonal), RIF1 (A300-569A, Bethyl Laboratories), γ-H2AX (05-636-1, Millipore), FLAG (F3165, Sigma), anti-acetylated lysine (9441, Cell Signaling), H2A (ab18255, Abcam), NBS1 (A301-289A, Bethyl Laboratories) and NBS1-p-S343 (3001, Cell Signaling).

Transfection and siRNA

Cells were transfected using polyetherimide. HeLa cells were transfected with specific siRNA or control siRNA using Lipofectamine 2000. The siRNAs were purchased from GenePharma (Shanghai). The gene targeting sequences were as follows: siCBP, GCAAGAAUGCCAAGAAGAAtt; siBRCA1, CAGCUACCCUUCCAUCAUAtt.

Immunoprecipitation and Western blotting

NETN buffer (20 mM Tris–HCl [pH 8.0], 100 mM NaCl, 1 mM EDTA and 0.5% Nonidet P-40) was used to lyse HeLa cells or 293T cells by rotation at 4°C for 20 min. After the removal of cell debris by centrifugation (14 000 rpm for 10 min), the soluble fractions were collected and incubated with S protein agarose (Merck-Millipore) for 3 h at 4°C. S protein beads were washed three times with NETN buffer and boiled with 2× SDS loading buffer at 100°C for 8 min. The samples were then subjected to SDS-PAGE and immunoblotting with specific antibodies.

GST Pull-Down assay

The GST pull-down assay was performed as previously described. GST or GST fusion proteins were expressed and

purified from BL21. After sonication, proteins were purified with glutathione Sepharose 4B beads. The samples were analyzed by western blot with the indicated antibodies.

In vitro acetylation and deacetylation assays

53BP1 was acetylated *in vitro* as previously described (48). Briefly, GST and GST-Tudor-UDR were purified from *E. coli*, and SFB-CBP-HAT was purified from 293T cells. The acetylation reaction was carried out in HAT buffer (50 mM Tris–HCl [pH 8.0], 0.1 mM EDTA, 1 mM DTT and 10% glycerol) for 1 h at 30°C. The reactions were resolved by SDS-PAGE and analyzed by Coomassie brilliant blue staining and western blotting.

Colony formation assay

The cells were treated as indicated and plated in 60-mm dishes. After 14 days of treatment, the cells were washed with phosphate-buffered saline (PBS) and stained with 0.1% Coomassie brilliant blue in 10% ethanol for 30 min at room temperature. The stained dishes were washed with water, and the colonies were counted.

Immunostaining

HeLa cells were cultured on coverslips and transfected with the indicated siRNA using a liposomal transfection reagent. Forty-eight hours after transfection, the cells were irradiated with the indicated dose of IR. After incubation for the indicated time, the cells were fixed in 4% formaldehyde at room temperature for 15 minutes and permeabilized with 0.25% Triton X-100 in 10 mM PBS for 5 min. After blocking non-specific antibody binding sites with 1% bovine serum albumin in 10 mM PBS, the cells were incubated with the indicated antibody at room temperature for 60 min. After three washes with PBS, the secondary antibody was added, and the cells were placed in the dark at room temperature for 30 min. They were then stained with DAPI to visualize nuclear DNA. Coverslips were placed on the glass slides with anti-fade solution, and the results were visualized using a ZEISS fluorescence microscope.

NHEJ assay

The NHEJ repair efficiency assay was described previously (49). Briefly, cells were transfected with linearized pcDNA3.1/puromycin (Invitrogen) and the pEGFP-C1 plasmid. Thirty-six hours later, the cells were collected, counted and plated on two plates. The transfection efficiency was determined and normalized to EGFP expression. After incubation for 14 days, the cells were washed with PBS and stained with 0.1% Coomassie brilliant blue in 10% ethanol for 30 min at room temperature. The stained dishes were washed with water, and the colonies were counted. Random plasmid integration events were normalized for transfection and plating efficiencies.

RESULTS

53BP1 is an acetylated protein, and 53BP1 acetylation is dramatically repressed by IR

Post-translational modifications of 53BP1, such as phosphorylation, are critical for modulating 53BP1-mediated DDR function and dictating the DSB repair pathway by antagonizing BRCA1 through the recruitment of PTIP/Artemis and RIF1/Rev7 (6). Protein acetylation is important in many cellular processes, including DDR, but it remains unclear whether acetylation is involved in modulating 53BP1 function. Therefore, we determined whether 53BP1 could be acetylated *in vivo*. As shown in Figure 1A and B, endogenous 53BP1 was confirmed to be acetylated *in vivo* based on immunoprecipitation with an anti-acetylated-lysine or anti-53BP1 antibody and western blotting with an anti-53BP1 or anti-acetylated-lysine antibody, respectively. As 53BP1 plays central roles in DNA DSB repair, we examined whether IR-induced DNA DSBs affect 53BP1 acetylation. Interestingly, 53BP1 acetylation was dramatically repressed by IR-induced DNA DSBs (Figure 1C).

Next, we identified the acetyltransferase responsible for the acetylation of 53BP1. Upon transfection of certain acetyltransferases, such as p300, CBP, PCAF, Tip60, Gcn5, HAT1, MYST1 and MYST2, into 293A cells stably expressing 53BP1, we found that only CBP acetylated 53BP1 *in vivo* (Figure 1D). Importantly, CBP acetylated 53BP1 in a dose-dependent manner (Figure 1E). Co-immunoprecipitation (co-IP) assays confirmed the interaction between 53BP1 and CBP (Supplementary Figure S1A). Ectopic expression of wild type (WT) or catalytically inactive (HAT domain) CBP and FLAG-tagged 53BP1 confirmed that CBP-mediated acetylation of 53BP1 depended on its HAT activity (Figure 1F). Meanwhile, *in vitro* acetylation analysis indicated that 53BP1 acetylation was dependent on CBP-HAT domain activity (Figure 1G). Moreover, we found that 53BP1 acetylation was significantly repressed in CBP-depleted cells, suggesting that CBP is essential for acetylating 53BP1 *in vivo* (Figure 1H). All these data show that CBP is sufficient and required for 53BP1 acetylation *in vivo*.

Acetylation of 53BP1 abolishes IR-induced 53BP1 foci formation

It is interesting that 53BP1 acetylation is dramatically repressed in response to DNA DSBs. 53BP1 is a key regulator of DSB processing and repair by NHEJ; thus, we wondered whether acetylation regulates DSB signaling. 53BP1 is one of the proteins initially recruited to DNA damage sites, and this recruitment is extremely important for 53BP1 function and the choice of DSB repair pathway. Therefore, we first ascertained whether CBP-mediated acetylation of 53BP1 affects its recruitment to DSBs. HeLa cells were transfected with CBP-WT or catalytically inactive CBP-Y1503F for 36 h and then mock-treated or treated with 5 Gy of IR. Surprisingly, CBP-WT significantly repressed IR-induced 53BP1 foci formation, but CBP-Y1503F had no effect (Figure 2A, B and Supplementary Figure S1B). In addition, neither CBP-WT nor CBP-Y1503F had a significant effect on γ-H2AX foci formation and 53BP1 protein level (Figure 2A andB, Supplementary Figure S1B and C).

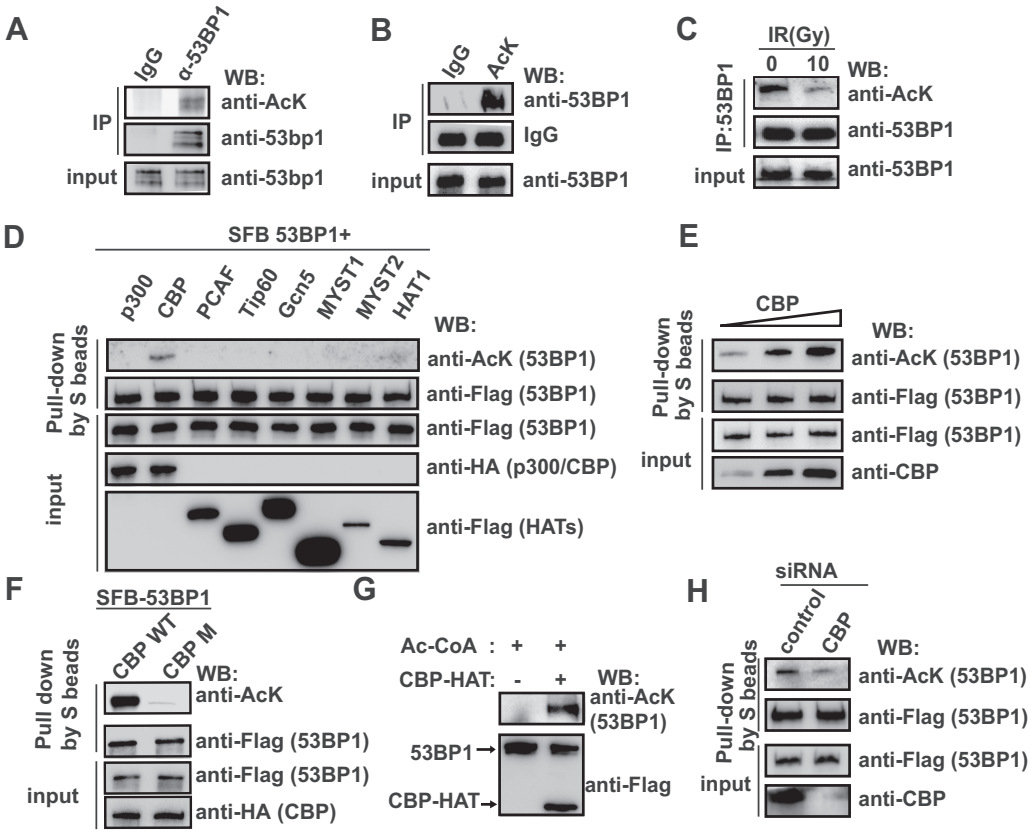

Figure 1. 53BP1 is an acetylated protein, and its acetylation is dramatically repressed by ionizing radiation (IR). (**A**) 53BP1 was acetylated *in vivo*. HeLa cell lysates were immunoprecipitated with rabbit IgG and an anti-AcK (acetylated lysine) antibody. Western blot was performed with the indicated antibodies. (**B**) Endogenous 53BP1 was acetylated *in vivo*. HeLa cells were lysed, and immunoprecipitations were performed with rabbit IgG and a 53BP1 antibody. Western blot was performed with the indicated antibodies. (**C**) 53BP1 acetylation was repressed by IR. HeLa cells were treated with IR (10 Gy) and then incubated for 1 hour. The acetylation level was assessed by western blot with the indicated antibodies. (**D**) CBP acetylated 53BP1 *in vivo*. SFB-53BP1 was stably expressed in HEK293A cells. The indicated HATs were transfected into cells stably expressing 53BP1. The acetylation signal was detected by western blot with the indicated antibodies. (**E**) CBP acetylated 53BP1 in a dose-dependent manner. Increasing amounts of CBP were transfected into cells stably expressing SFB-53BP1. The acetylation signal was detected by western blot with the indicated antibodies. (**F**) CBP acetylation of 53BP1 depended on its HAT activity. HA-tagged CBP-WT and an inactive mutant (CBP-Y1503F) were transfected into cells stably expressing SFB-53BP1. Western blot was performed with the indicated antibodies. (**G**) CBP-HAT acetylated 53BP1 *in vitro*. SFB-53BP1 and Flag-CBP-HAT (residues 1100–1712) were purified from 293T cells, and an *in vitro* acetylation assay was performed. The acetylation signal was detected by western blot with the indicated antibodies. (**H**) 53BP1 acetylation was diminished in CBP-depleted cells. CBP was knocked down with siRNA in 293A cells stably expressing 53BP1, and western blot was performed with the indicated antibodies.

Previous investigations showed that the tandem Tudor domain and the UDR motif of 53BP1 were sufficient and required for IR-induced foci formation; therefore, we hypothesized that the potential sites of CBP-mediated acetylation were within this region. Indeed, the Tudor-UDR domain (residues 1052–1700), which contains the tandem Tudor domain and UDR motif, was acetylated *in vivo* (Supplementary Figure S1D).

Ectopic expression of WT or catalytically inactive (HAT domain) CBP and SFB-Tudor-UDR, confirmed that the Tudor-UDR domain is acetylated by CBP *in vivo* (Figure 2C). Moreover, C646, a selective inhibitor of p300/CBP, clearly repressed the acetylation of Tudor-UDR (Figure 2D). To confirm these findings, *in vitro* acetylation assays were performed by incubating purified *E. coli*-expressed GST or GST-tagged Tudor-UDR with the acetyltransferase (HAT) domain of CBP (residues 1100–1712). The Tudor-UDR domain was indeed acetylated by CBP *in vitro* (Figure 2E).

53BP1 is acetylated at K1626/1628 by CBP

To identify the 53BP1 acetylation sites, stably expressed 53BP1 was purified from 293A cells and analyzed by LC–MS/MS. Two acetylated lysine residues (K1626/1628) within 53BP1 were identified *in vivo* (Figure 3A). These residues are located in the UDR motif of 53BP1 and are conserved from human to yeast (Figure 3B), suggesting they may have an important function.

To confirm that K1626/1628 are the major acetylated residues of 53BP1, they were replaced with arginine by mutagenesis. As shown in Figure 3C, the acetylation of the 53BP1-K1626/1628R mutant was significantly decreased compared to that of WT 53BP1, suggesting that K1626/1628 are the major acetylation sites of 53BP1.

To further prove acetylation of 53BP1 at K1626/1628 *in vivo*, an antibody that specifically recognizes AcK1626/1628–53BP1 was generated. The specificity of the antibody against AcK1626/1628–53BP1 was verified

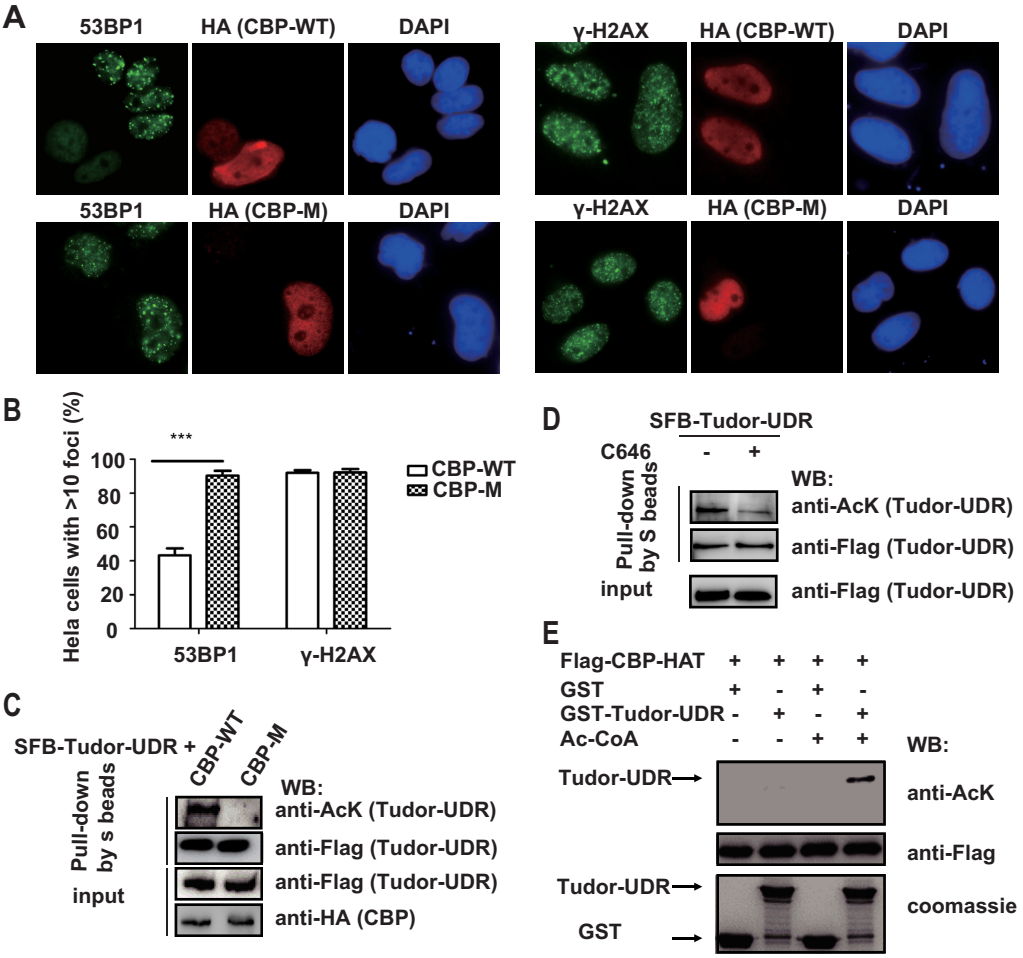

Figure 2. 53BP1 acetylation decreases IR-induced 53BP1 foci formation. (**A**) Overexpressing CBP abolished 53BP1 foci formation. HA-CBP-WT and HA-CBP-Y1503F constructs were transfected into HeLa cells, which were then treated with IR (5 Gy) and incubated for 1 h before immunofluorescence analysis. (**B**) Histogram of the percentage of cells with >10 53BP1 or γ-H2AX foci. Over 100 cells were counted. Data are presented as the mean ± SEM ($n = 3$, $^{***}P < 0.001$). (**C**) CBP acetylated the Tudor-UDR domain of 53BP1. HEK293T cells were transfected with SFB-Tudor-UDR and HA-CBP-WT or HA-CBP-Y1503F. Western blot was performed with the indicated antibodies. (**D**) The CBP inhibitor reduced the acetylation of the Tudor-UDR domain. HeLa cells stably expressing SFB-Tudor-UDR were treated with or without 10 μM C646 for 12 h. Western blot was performed with the indicated antibodies. (**E**) CBP-HAT acetylated the Tudor-UDR domain *in vitro*. GST or GST-Tudor-UDR purified from *E. coli* was incubated with SFB-CBP-HAT in HAT buffer for 1 h. Then, the reaction samples were boiled with SDS loading buffer and subjected to western blot with the indicated antibodies.

by dot blot assay (Figure 3D) and by its ability to recognize 53BP1-WT rather than the 53BP1-K1626/1628R mutant (Figure 3E). K1626/1628 were acetylated by CBP in a dose-dependent manner (Figure 3F). We further investigated whether 53BP1 K1626/1628 acetylation is regulated by DNA damage. Consistent with previous results, IR-induced DNA DSBs significantly repressed 53BP1 K1626/1628 acetylation (Figure 3G). To evaluate the percentage of acetylation occupancy on K1626/1628 of 53BP1, we performed the immunofluorescence experiment by using K1626/1628ac antibody. As expected, most HeLa cells are 53BP1-K1626/1628ac positive compare with 53BP1 knockout cells, suggesting that the acetylation occupancy on K1626/1628 is very high percentage (Supplementary Figure S2A). Taken together, we concluded that 53BP1 is acetylated at residues K1626/1628 by CBP and that DNA damage negatively regulates this process.

K1626/1628 acetylation negatively regulates 53BP1 foci formation

It was surprising that CBP-mediated acetylation of 53BP1 dramatically repressed 53BP1 foci formation (Figure 2A); thus, we wondered whether 53BP1 K1626/1628 acetylation was responsible for this result. We generated the 53BP1-K1626/1628R mutant in the Tudor-UDR domain, which mimics un-acetylated 53BP1, and the 53BP1-K1626/1628Q mutant in the Tudor-UDR domain, which mimics hyperacetylated 53BP1. We compared foci formation in HeLa cells stably expressing Tudor-UDR-WT, Tudor-UDR-K1626/1628R or Tudor-UDR-K1626/1628Q. Compared with untreated cells, there was no difference between Tudor-UDR-K1626/1628R and Tudor-UDR-WT upon DNA damage (Figure 4A, B and Supplementary Figure S2B). However, the K1626/1628Q mutant, which mimics the hyperacetylated Tudor-UDR domain, significantly inhibited 53BP1 foci formation compared with

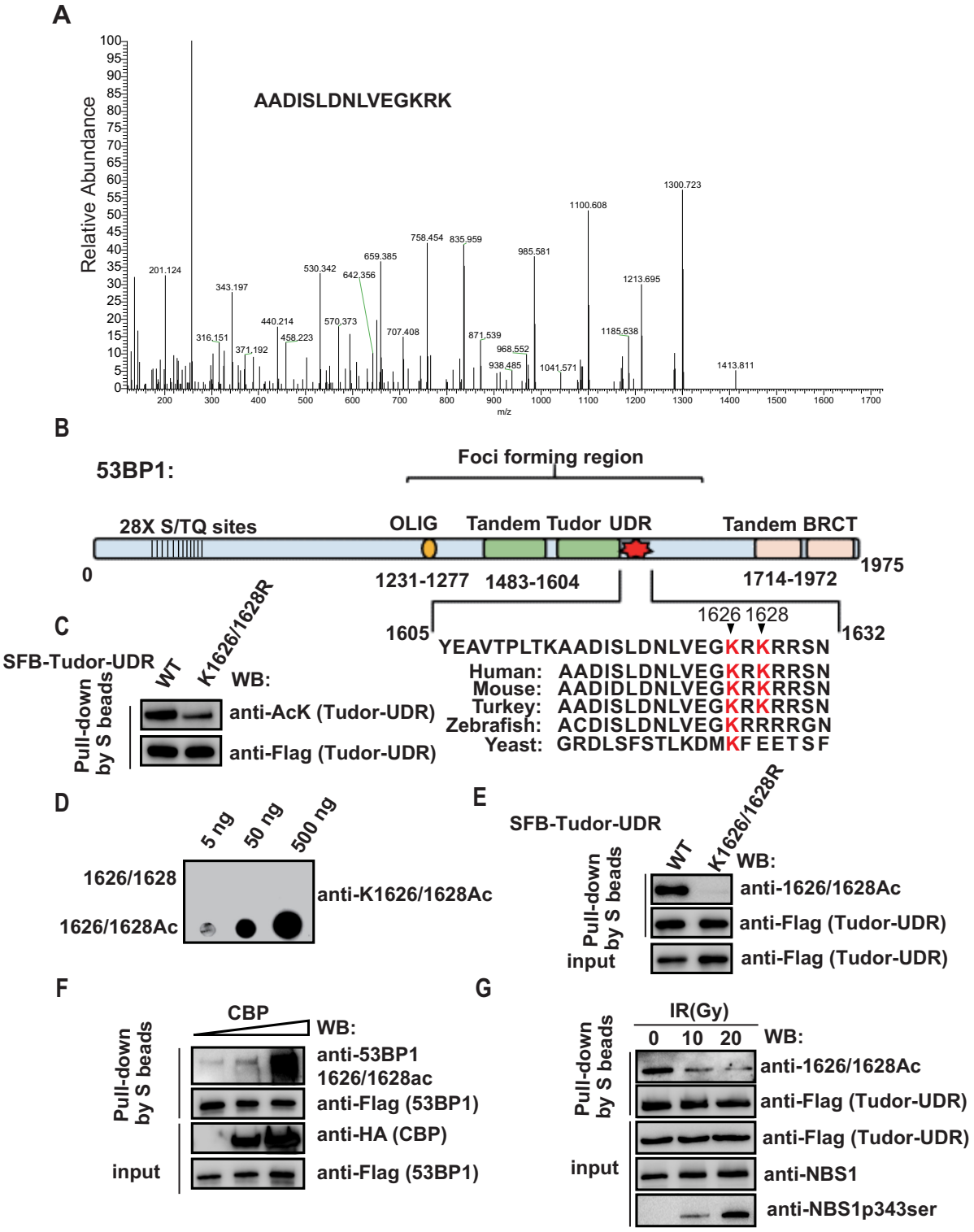

Figure 3. 53BP1 is acetylated at K1626/1628 by CBP. (**A**) 53BP1 acetylation was analyzed by mass spectrometry (MS). SFB-53BP1 was purified from stable 293T cells prior to MS analysis. (**B**) Alignment of K1626/1628 in 53BP1 orthologues. (**C**) Mutation of K1626/1628 significantly decreased the acetylation of the Tudor-UDR domain. SFB-Tudor-UDR and K1626/1628R-Tudor-UDR were transfected into 293T cells. SFB-Tudor-UDR was pulled down from cell lysates using S protein beads and immunoblotted with the indicated antibodies. (**D**) The specificity of the antibody against AcK1626/1628–53BP1 was verified by dot blot assays. The nitrocellulose membrane was spotted with the indicated amounts of unacetylated or acetylated 53BP1 peptides and immunoblotted with the AcK1626/1628–53BP1 antibody. (**E**) Verification of the specificity of the AcK1626/1628–53BP1 antibody. SFB-53BP1-WT or SFB-53BP1-K1626/1628R was transfected into 293T cells. SFB-53BP1 was pulled down from cell lysates using S protein beads and immunoblotted with the indicated antibodies. (**F**) CBP acetylated 53BP1 at K1626/1628. Increasing amounts of HA-CBP were transfected into cells stably expressing SFB-53BP1, and 53BP1 K1626/1628 acetylation was detected with the AcK1626/1628–53BP1 antibody. (**G**) IR repressed 53BP1 acetylation at K1626/1628. Cells stably expressing SFB-53BP1 were treated with increasing doses of IR, incubated for 2 h, collected and lysed for acetylation analysis. Anti-NBS1-p343ser was used as a marker of DNA damage.

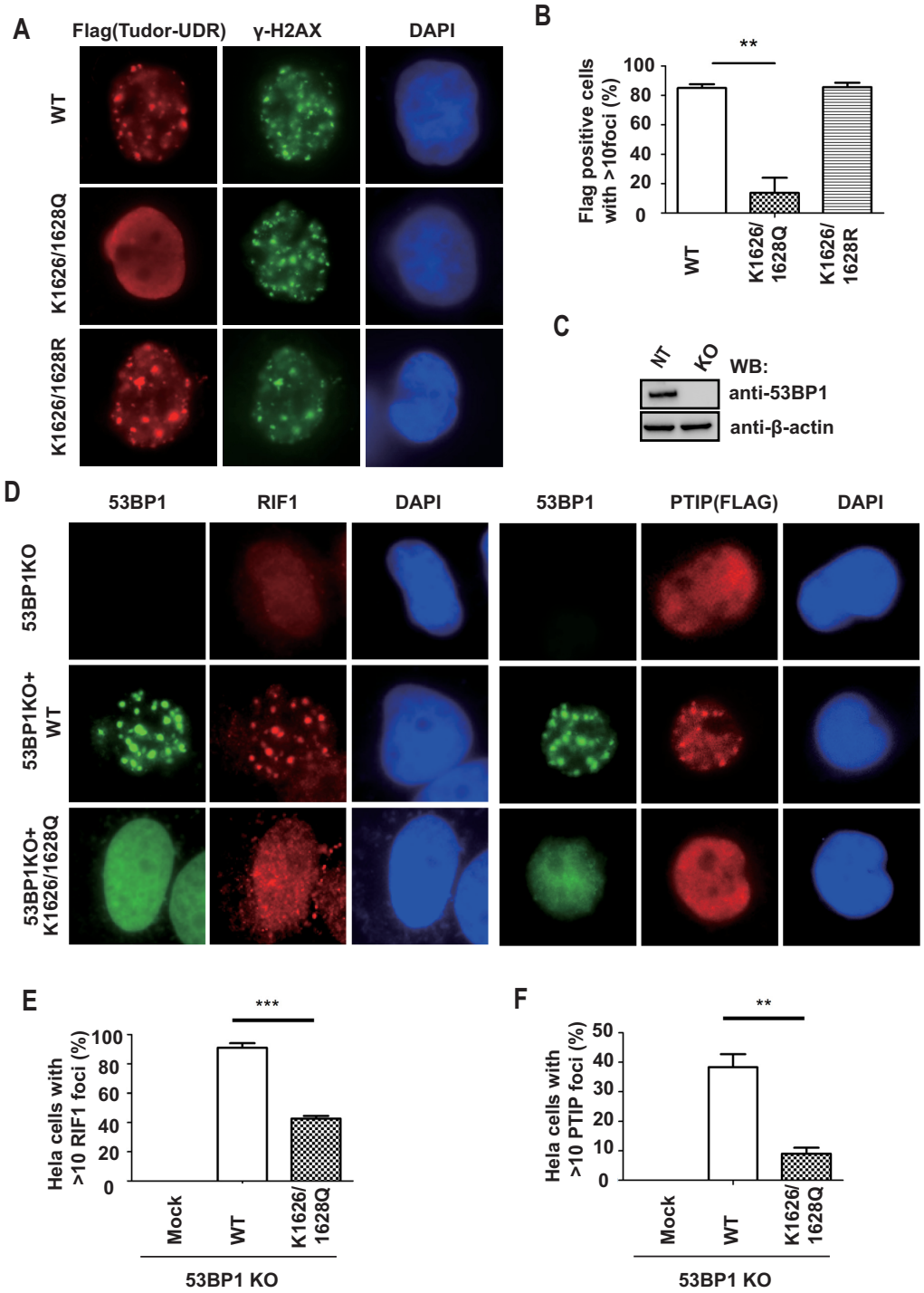

Figure 4. K1626/1628 acetylation negatively regulates 53BP1 foci formation. (**A**) K1626/1628 acetylation repressed foci formation of the Tudor-UDR domain. HeLa cells stably expressing SFB-Tudor-UDR-WT, SFB-Tudor-UDR-K1626/1628R, or SFB-Tudor-UDR-K1626/1628Q were treated with IR (5 Gy). After incubation for 1 hour, the cells were subjected to immunofluorescence. (**B**) Histogram of the percentage of cells with >10 IRIF of the Tudor-UDR domain. Over 100 cells were counted. Data are presented as the mean ± SEM ($n = 3$, $^{**}P < 0.01$). (**C**) Western blot confirmed 53BP1 expression in 53BP1-knockout and control cells. (**D**) 53BP1 K1626/1628 acetylation repressed PTIP/RIF1 foci formation. GFP-53BP1-WT or the GFP-53BP1-K1626/1628Q mutant was reconstituted in 53BP1-knockout cells. 53BP1 and PTIP or RIF1 foci formation was analyzed 1 hour after IR (5 Gy) treatment. (**E**, **F**) Quantification of PTIP and RIF1 foci formation with the indicated 53BP1 constructs. Data are presented as the mean ± SEM ($n = 3$, $^{***}P < 0.001$, $^{**}P < 0.01$).

Tudor-UDR-WT (Figure 4A, B and Supplementary Figure S2B). The same results were observed upon reconstituting full length 53BP1 and 53BP1 K1626/1628Q in 53BP1-knockout cells (Supplementary Figure S2C and D). These data suggested that the K1626/1628 acetylation status of 53BP1 is critical for its foci formation ability.

Since ATM-mediated phosphorylation of 53BP1 at its N-terminal SQ/TQ motif directly recruits PTIP and RIF1 to promote NHEJ, we investigated whether these factors are affected by 53BP1 acetylation. After reconstituting GFP-53BP1-WT and GFP-53BP1-K1626/1628Q in 53BP1-knockout cells, PTIP and RIF1 foci formation were detected upon IR treatment. As expected, 53BP1-knockout cells and GFP-53BP1-K1626/1628Q-reconstituted cells showed significant disruption of PTIP and RIF1 foci formation (Figure 4C–F). GFP-53BP1-WT-reconstituted cells efficiently recovered PTIP and RIF1 foci formation (Figure 4C–F).

Acetylation of K1626/1628 inhibits the binding between 53BP1 and H2Aub

Previous studies revealed that the accumulation of 53BP1 at DSBs requires recognition of H4K20me2 via the tandem Tudor-UDR domain and of H2A via the UDR motif, a C-terminal extension of the Tudor domain. In addition, 53BP1 oligomerization is critical for its recruitment to DSBs.

To better understand the mechanism by which acetylation represses 53BP1 foci formation, we ascertained which step is affected. First, we determined whether K1626/1628 acetylation alters 53BP1 oligomerization. SFB-Tudor-UDR-WT, SFB-Tudor-UDR-K1626/1628R, or SFB-Tudor-UDR-K1626/1628Q was used to pull-down Myc-Tudor-UDR-WT, Myc-Tudor-UDR-K1626/1628R, or Myc-Tudor-UDR-K1626/1628Q, respectively, but there were no differences in the oligomerization of WT 53BP1, hypoacetylated 53BP1 and hyperacetylated 53BP1 (Figure 5A). Next, we further explored whether the acetylation status of 53BP1 affects the recognition of H4K20me2. Biotin-labeled H4K20me2 peptide was used to pull down GST, GTS-Tudor-UDR-WT or GST-Tudor-UDR-K1626/1628Q, which mimics hyperacetylated 53BP1. There were no differences in the binding between the Tudor-UDR domain and the H4K20me2 peptide (Figure 5B). Considering that K1626/1628 is located in the UDR domain of 53BP1, which is required for the recognition of modified nucleosomes, we wondered whether K1626/1628 acetylation affects the interaction of 53BP1 with chromatin. Daniel Durocher's group has observed a UDR-dependent interaction between 53BP1 and histones H2A, H3 and H4 (36–38). We reproduced this observation in GST pull-down assays. Moreover, we found that the hyperacetylated UDR motif almost completely disrupted the interaction between 53BP1 and H2Aub or H2A, suggesting that acetylation of the UDR motif is extremely important for regulating the recruitment of 53BP1 to chromatin (Figure 5C). We confirmed this observation *in vivo* (Figure 5D). Moreover, C646, a potent inhibitor of CBP/p300, increased the interaction between H2A and Tudor-UDR-WT but had no effect on the interaction between H2A and Tudor-UDR-K1626/1628Q, suggesting that this interaction was influenced by acetylation of the UDR motif (Supplementary Figure S3). These data suggested that CBP-mediated 53BP1 K1626/1628 acetylation has no effect on oligomerization and H4K20me2 recognition, but is critical for regulating the interaction between 53BP1 and nucleosomes.

To further confirm the effect of K1626/1628 acetylation on the interaction between H2A and 53BP1, K1626/1628 was acetylated *in vitro*. Acetylated K1626/1628, which is within the UDR motif, significantly reduced the interaction between 53BP1-Tudor-UDR and H2A (Figure 5E). To further confirm that the acetylation status of the UDR motif is critical for regulating the endogenous association of 53BP1 and H2A *in vivo*, endogenous co-IP assays were performed using a 53BP1 antibody in the presence or absence of CBP depletion. As shown in Figure 5F, CBP depletion reduced K1626/1628 acetylation but enhanced the interaction between 53BP1 and H2A.

The complex structure of 53BP1-UDR and an H2AK15-ubiquitinated/H4K20-dimethylated nucleosome core particle (NCP) was drawn from PDB 5KGF [PMID 27462807]. 53BP1-UDR interacts with the NCP mainly through an acidic/negatively charged patch formed by H2A and H2B using several basic/positively charged residues, including K1626 and K1628 [PMID 27462807] (Figure 5G). The positively charged 53BP1-UDR K1626 residue interacts with the negatively charged H2A D90/E91/E92 and H2B E105 residues, while K1628 interacts with H2A E61/E64 (Figure 5H). The structure revealed that the acetylation of 53BP1-UDR K1626/1628 neutralizes the positive charge, thereby weakening the interaction between 53BP1-UDR and the NCP.

53BP1 K1626/1628 acetylation in tightly regulated by HDAC2

Acetylation is a highly dynamic post-translational modification, and the balance between acetylation and deacetylation plays critical roles in modulating protein function. We found that TSA significantly increased 53BP1 acetylation in a dose-dependent manner, implying that HDACs may be involved in deacetylating 53BP1 (Supplementary Figure S4A). We found that 53BP1 K1626/1628 acetylation significantly decreased with increasing HDAC2 expression and slightly decreased with increasing HDAC1 expression (Figure 6A). Moreover, HDAC2 depletion led to a clear increase in 53BP1 K1626/1628 acetylation level (Figure 6B). It was interesting that HDAC2 could regulate 53BP1 K1626/1628 acetylation; we further showed that endogenous 53BP1 specifically interacted with endogenous HDAC2 (Figure 6C).

It is important to know how 53BP1 acetylation is repressed by IR. We determined that interaction between 53BP1 and HDAC2 was induced by DNA damage and was mainly dependent on ATM kinase (Figure 6D). ATM preferentially phosphorylates many downstream substrates at SQ/TQ sites to trigger cellular responses after DNA damage. HDAC2 contains an SQ (S4) site at the extreme N-terminus, and replacing the serine with alanine disrupted the interaction of 53BP1 with HDAC2 (Fig-

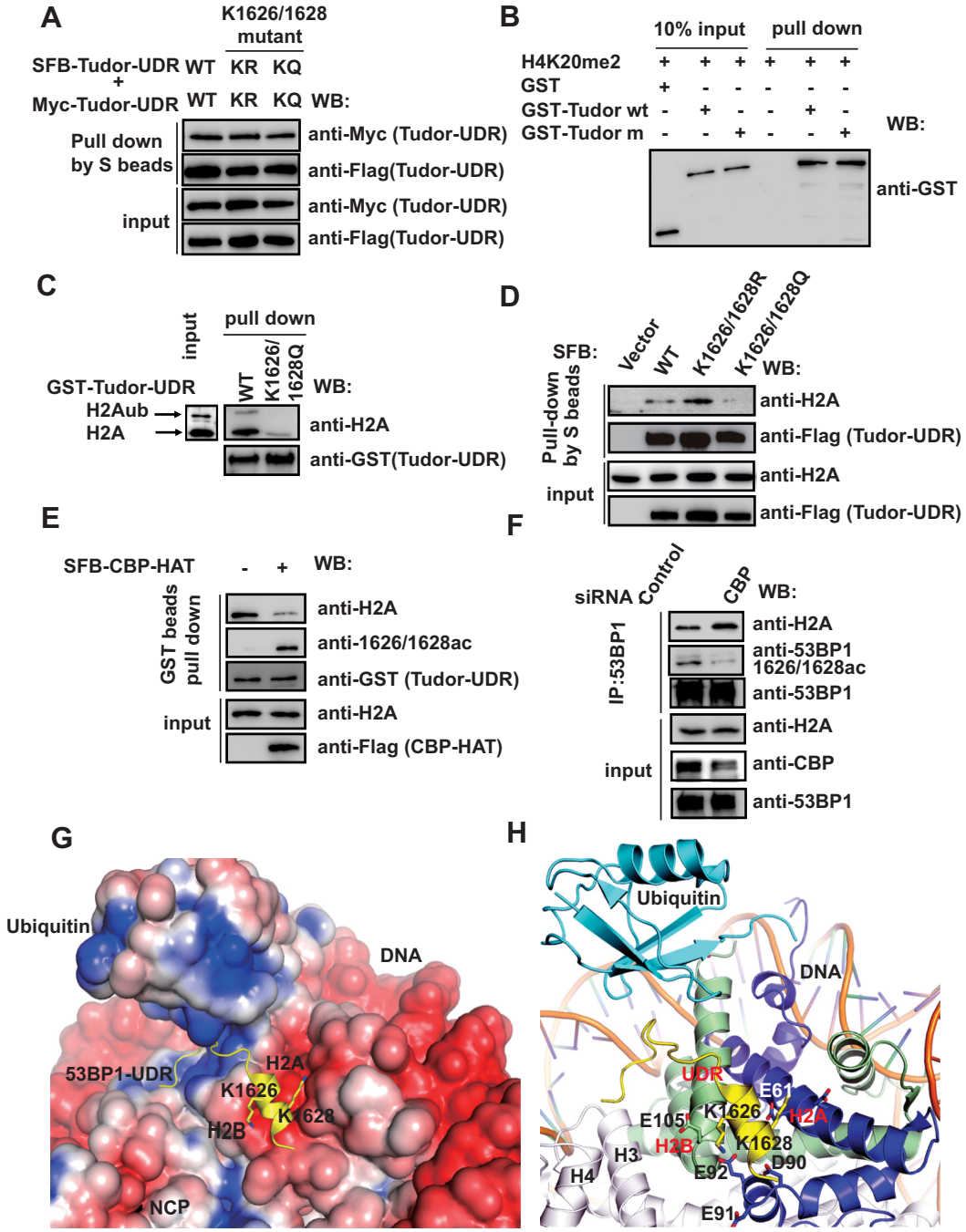

Figure 5. K1626/1628 acetylation inhibits the binding between 53BP1 and H2A. (**A**) K1626/1628 acetylation did not affect oligomerization of the Tudor-UDR domain. SFB-Tudor-UDR-WT, SFB-Tudor-UDR-K1626/1628R or SFB-Tudor-UDR-K1626/1628Q was co-transfected with Myc-Tudor-UDR-WT, Myc-Tudor-UDR-K1626/1628R or Myc-Tudor-UDR-K1626/1628Q, respectively. SFB-Tudor-UDR was pulled down from cell lysates using S protein beads and immunoblotted with the indicated antibodies. (**B**) K1626/1628 acetylation did not affect the interaction between H4K20me2 and the Tudor-UDR domain. Biotin-labeled H4K20me2 peptides pulled down *E. coli*-expressed GST, GST-Tudor-UDR-WT or GST-Tudor-UDR-K1626/1628 using streptavidin agarose. (**C**) K1626/1628 acetylation inhibited the interaction between the Tudor-UDR domain and H2A in the GST pull-down assay. *E.coli*-purified GST, GST-Tudo-UDRr-WT or GST-Tudor-UDR-K1626/1628 was pulled down in the chromatin-enriched fraction of IR-treated (10Gy) HeLa cells. (**D**) The K1626/1628 acetylation mimic mutant disrupted the interaction between H2A and the Tudor-UDR domain. HEK293T cells were transfected with the indicated plasmid for 36 hours and treated with IR (10 Gy). Then, pull-down assays were conducted using S protein beads. (**E**) CBP-mediated K1626/1628 acetylation disrupted the interaction between Tudor-UDR and H2A. *Escherichia coli*-purified GST-Tudor-UDR was incubated with or without IR-treated (10 Gy) 293T-purified SFB-CBP-HAT in HAT buffer for 1 h. Then, samples were subjected to pull-down assays in NETN buffer and chromatin-enriched cell lysates as described in the procedures. (**F**) siRNA-mediated CBP knockdown enhanced the interaction between endogenous 53BP1 and H2A. Control siRNA or CBP siRNA was transfected twice into HeLa cells for 72 h and treated with 10 Gy IR. After releasing for 6 h, the cells were lysed in RIPA buffer and co-immunoprecipitated with the 53BP1 antibody. (**G**, **H**) 53BP1-UDR interacted with the NCP mainly through an acidic/negatively charged patch formed by H2A and H2B using several basic/positively charged residues, including K1626 and K1628.

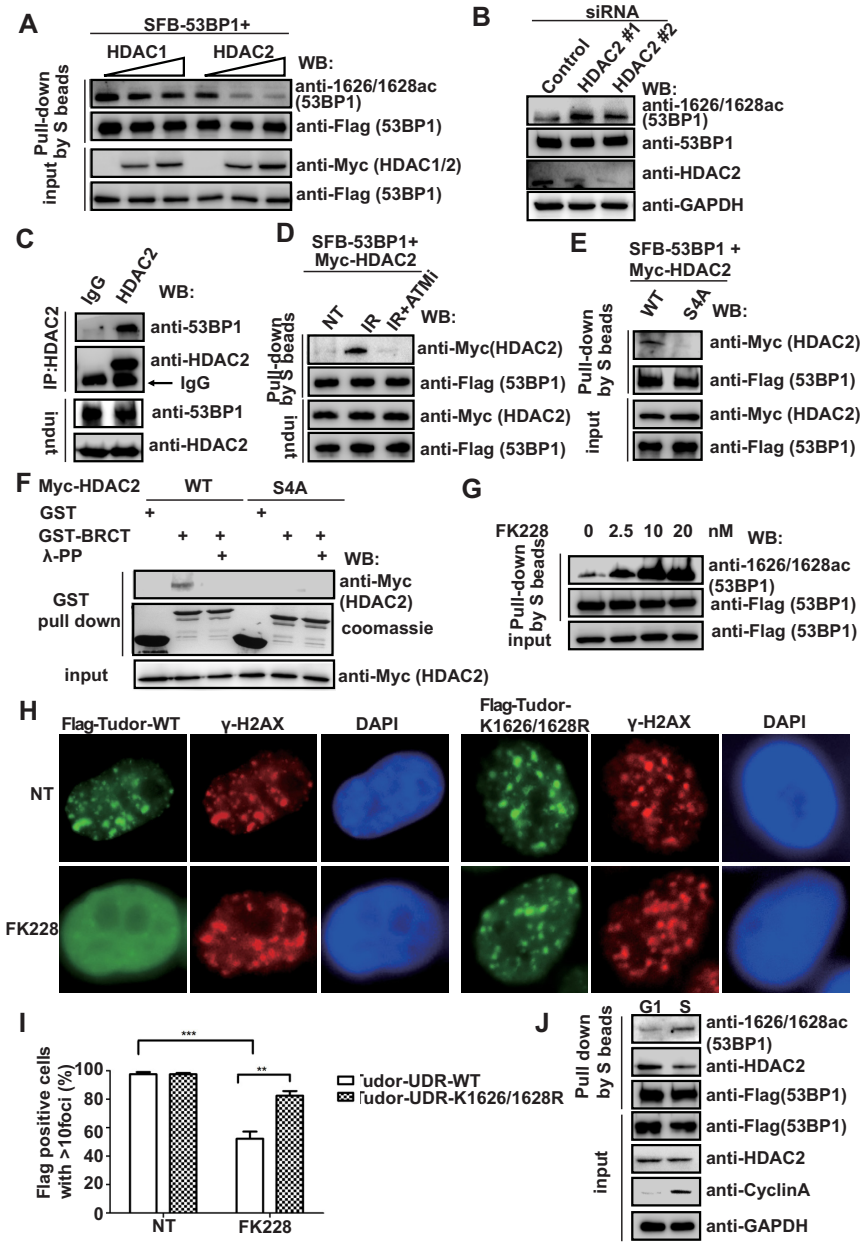

Figure 6. 53BP1 K1626/1628 acetylation is tightly regulated by HDAC2. (**A**) HDAC2 specific deacetylates 53BP1 at K1626/1628. HEK293A cells stably expressing SFB-53BP1 were transfected with increasing amounts of HDAC1 or HDAC2. Then, K1626/1628 acetylation was assessed with the specific AcK1626/1628–53BP1 antibody. (**B**) Depletion of HDAC2 increases 53BP1 K1626/1628 acetylation. HeLa cells transfected with control or HDAC2 siRNA were harvested and immunoblotted with the indicated antibodies. (**C**) Endogenous HDAC2 interacted with endogenous 53BP1. HeLa cells were lysed with NETN buffer, and the cell lysates were subjected to immunoprecipitation with rabbit IgG or anti-HDAC2 antibody. After incubation with Protein A agarose, the samples were analyzed by western blot with the indicated antibodies. (**D**) The interaction of 53BP1 with HDAC2 was induced by DNA damage, which is mainly dependent on ATM kinase. Myc-HDAC2 was transfected into HEK293A cells stably expressing SFB-53BP1, which were then treated with 10 μM ATM inhibitor (KU-55933) for 2 h before IR (10 Gy) treatment. After incubation for 2 h, the cells were lysed with RIPA buffer, and co-IP assays were performed with the indicated antibodies. (**E**) The interaction between HDAC2 and 53BP1 was dependent on HDAC2-S4 phosphorylation. Myc-HDAC2-WT or Myc-HDAC2-S4A was transfected into HEK293A cells stably expressing SFB-53BP1, which were then treated with IR (10 Gy). After incubation for 2 hours, co-IP assays were conducted with the indicated antibodies. (**F**) The tandem BRCT motifs mediated the interaction between 53BP1 and phosphorylated HDAC2. Lysates from cells expressing exogenous Myc-HDAC2-WT or Myc-HDAC2-S4A that were treated with IR (10 Gy) and λ protein phosphatase or mock control were incubated with beads coated with *E. coli*-expressed GST or GST-53BP1-BRCTs293T. (**G**) FK228 increased 53BP1 K1626/1628 acetylation. HEK293A cells stably expressing SFB-53BP1 were treated with increasing concentrations of FK228 (specific inhibitor of HDAC1 and HDAC2 at low concentration), and K1626/1628 acetylation was analyzed by western blot. (**H**) FK228 specifically repressed the foci formation of WT 53BP1 but not of the 53BP1-K1626/1628R mutant. HeLa cells stably expressing SFB-53BP1-or and SFB-53BP1-K1626/1628R were treated with FK228 (2.5 nM) for 24 h. Then, after IR (5 Gy) treatment and a 2-h incubation, cells were subjected to immunofluorescence analysis. (**I**) Histogram of the percentage of cells with >10 IRIF. Over 100 cells were counted. Data are presented as the mean ± SEM ($n = 3$, $^{**}P < 0.01$, $^{***}P < 0.001$). (**J**) The 53BP1 K1626/1628 acetylation and 53BP1/HDAC2 interaction is cell cycle–regulated. HeLa cells stably expressed 53BP1 were synchronized by double thymidine block, and then released in fresh medium without thymidine and collected in G1 and S phase. Immunoprecipitation and immunoblotting experiments were performed using antibodies as indicated.

ure 6E), suggesting that this interaction is phosphorylation dependent. 53BP1 contains two BRCT domains, which are phosphoprotein-binding domains. To further evaluate whether the interaction between 53BP1 and HDAC2 is phosphorylation dependent, cell lysates were treated with λ protein phosphatase and subjected to a GST pull-down assay. The interaction between 53BP1 and HDAC2 was abolished after treatment with λ protein phosphatase, but HDAC2-S4A failed to interact with the BRCT domains of 53BP1 in the absence of λ protein phosphatase treatment (Figure 6F), suggesting that phosphorylation of HDAC2 at S4 is required for the 53BP1/HDAC2 interaction.

Importantly, the degree of 53BP1 K1626/1628 acetylation was markedly increased by FK228, a selective and relatively specific HDAC1 and HDAC2 inhibitor at low concentration (Figure 6G). We showed that 53BP1 acetylation is critical for its association with chromatin and foci formation; therefore, we questioned the effect of repressing the deacetylation of 53BP1. As expected, foci formation of 53BP1 and its downstream factor RIF1 was significantly reduced by FK228 (Supplementary Figure S4B and C), which markedly increased 53BP1 K1626/1628 acetylation (Figure 6G). Interestingly, FK228 inhibited only WT 53BP1 foci formation, not that of the 53BP1-K1626/1628R mutant (Figure 6H and I), suggesting that FK228 represses 53BP1 foci formation by regulating the K1626/1628 acetylation status.

Importantly, 53BP1 K1626/1628 acetylation was enriched in S phase but limited in G1 phase (Figure 6J), while the interaction between 53BP1 and HDAC2 increased in G1 phase and decreased in S phase (Figure 6J), suggesting that 53BP1 K1626/1628 acetylation was tightly regulated by HDAC2 not only in DNA damage response but also in cell cycle stages.

53BP1 K1626/1628 acetylation restores PARPi resistance in BRCA1-deficient cells by promoting DNA end resection and HR repair

It is interesting that 53BP1 K1626/1628 acetylation was tightly regulated in DNA damage response and cell cycle stages. 53BP1 is an important factor in DSB signaling for class switch recombination and is a key regulator of DSB processing and repair by NHEJ. 53BP1 K1626/1628 acetylation inhibits 53BP1 recruitment to DSBs by weakening the interaction between 53BP1-UDR and the NCP. We first investigated whether 53BP1 K1626/1628 acetylation affects 53BP1-mediated DNA repair ability. Compared with normal cells or 53BP1-WT-reconstituted cells, 53BP1-knockout cells and 53BP1-K1626/1628Q-reconstituted cells were more sensitive to IR (Figure 7A), suggesting that K1626/1628 acetylation impairs 53BP1-mediated DSB repair.

The recruitment of 53BP1 to damaged chromatin dictates the DSB repair pathway by promoting NHEJ-mediated DSB repair and preventing HR. Our data clearly showed that 53BP1 K1626/1628 acetylation represses its recruitment to DSBs; thus, we reasoned that K1626/1628 acetylation may prevent NHEJ and promote DNA end resection and HR. Indeed, reconstitution of 53BP1-WT, but not of the 53BP1-K1626/1628Q mutant, in 53BP1-knockout cells resensitized BRCA1-deficient cells to PARPi (Figure 7B). The efficiency of BRCA1 depletion is shown in Supplementary Figure S5A. PARPi sensitivity was restored in BRCA1-deficient cells by co-treatment with FK228 (Figure 7C), which significantly increased 53BP1 K1626/1628 acetylation and repressed WT 53BP1 foci formation but not that of the 53BP1 K1626/1628R mutant. These data indicated that K1626/1628 acetylation, which abolished 53BP1 foci formation and the interaction with H2A, was important for the function of 53BP1 in inhibiting HR-mediated repair.

To confirm that 53BP1 K1626/1628 acetylation restores PARPi resistance in BRCA1-deficient cells by promoting DNA end resection and HR, we analyzed RPA2 foci (marker of DNA end resection) and Rad51 foci (marker of HR repair) in cells depleted of both 53BP1 and BRCA1. Both RPA2 foci and Rad51 foci were restored by reconstitution of 53BP1-K1626/1628Q in BRCA1-deficient cells (Figure 7D–G). Moreover, NHEJ activity was significantly repressed while HR efficiency was promoted by the reconstitution of 53BP1-K1626/1628Q in 53BP1-knockout cells (Supplementary Figure S5B and S5C). These data clearly showed that 53BP1 K1626/1628 acetylation restores PARPi resistance in BRCA1-deficient cells by repressing NHEJ and promoting DNA end resection and HR-mediated repair.

DISCUSSION

53BP1 is a key regulator of DNA DSBs that promotes NHEJ repair and inhibits HR by antagonizing BRCA1 (6). Previous studies had also proposed that the acetylation histones, such as H4K16, inhibit 53BP1 recruitment DSBs (20,21,23,50). In this study, we provide evidence that CBP-mediated K1626/1628 acetylation of 53BP1 represses 53BP1 foci formation and abolishes PARPi sensitivity in BRCA1-deficient cells. Mechanistically, 53BP1 K1626/1628 acetylation disrupts the interaction between 53BP1 and nucleosomes; this acetylation is tightly regulated by ATM-dependent HDAC2 deacetylation. Thus, our findings reveal how acetylation regulates BRCA1 antagonism by 53BP1 and dictates the choice of DNA DSB repair pathway (Figure 8).

Protein acetylation, similar to phosphorylation and ubiquitination, is emerging as an important regulator of signal transduction in response to DNA damage (51,52). Numerous DNA repair proteins have been identified to undergo lysine acetylation, including MDC1, NBS1, ATM, TopBP1 and CtIP (22,53–56), indicating that the acetylation of DNA repair factors plays potential roles in the response to and repair of cellular DNA damage. We discovered that 53BP1 is acetylated *in vitro* and *in vivo* by CBP, which acetylates various non-histone proteins such as p53, Ku70 and PCNA (57).

Our data has shown that CBP acetylated 53BP1 and repressed its recruitment to DSBs (Figure 2). Therefore, the mass spectrometry analyses were performed to identify the acetylation residues in cells stably expressed 53BP1-Tudor-UDR, which is regarded as foci forming region of 53BP1. The mass spectrometry and further studies revealed that 53BP1-Tudor-UDR was acetylated at residues K1626/1628

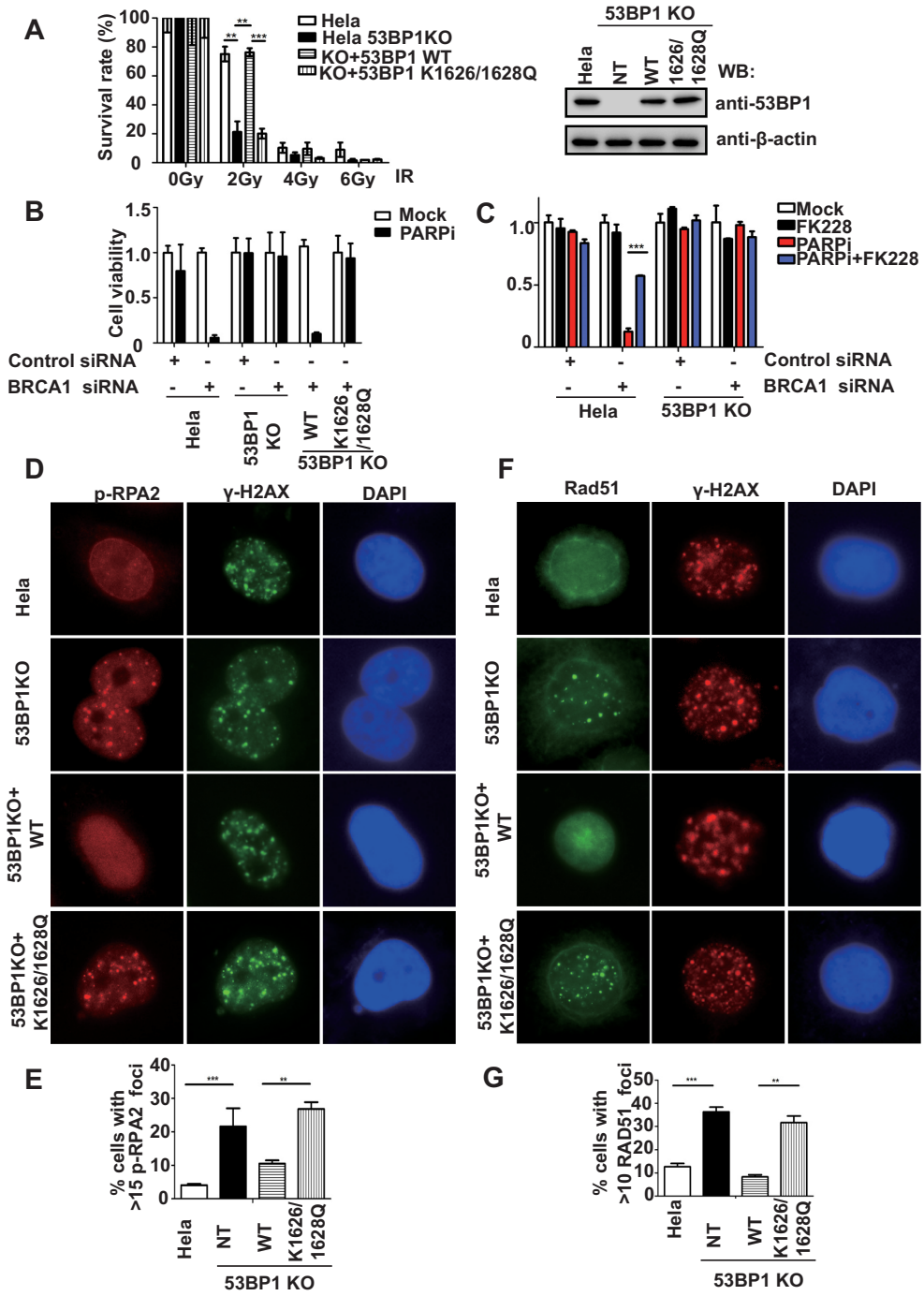

Figure 7. 53BP1 K1626/1628 acetylation restores PARPi resistance in BRCA1-deficient cells by promoting DNA end resection and HR. (**A**) Hyperacetylated 53BP1 caused IR sensitivity. 53BP1-WT or 53BP1-K1626/1628Q was reconstituted in 53BP1-knockout HeLa cells. The relative expression of each reconstituted protein is shown. The cell viability was assessed after the indicated IR treatment. The histogram shows the statistical analysis of the colony formation assay. Data are presented as the mean ± SEM ($n = 3$, $^{**}P < 0.01$, $^{***}P < 0.001$). (**B**) Hyperacetylated 53BP1 caused PARPi resistance in BRCA1-deficient cells. Hyperacetylated 53BP1 caused IR sensitivity. 53BP1-WT or 53BP1-K1626/1628Q was reconstituted in 53BP1-knockout HeLa cells. Control siRNA or BRCA1 siRNA was transfected twice into the indicated cells for 72 h, and cells were treated with control or 1 μM PARPi for 24 h. After 14 days, the colonies were counted, and the result are presented in the histogram. Data are presented as the mean ± SEM ($n = 3$, $^{**}P < 0.01$, $^{***}P < 0.001$). The BRCA1 knockdown efficiency is shown in Supplementary Figure S5A. (**C**) HeLa cells and 53BP1-knockout cells were transfected with control siRNA or BRCA1 siRNA for 72 h as indicated. The cells were treated with FK228 (2.5 nM) for 12 h prior to treatment with PARPi (1 μM) for 24 h. The colony formation results are presented in the histogram. Data are presented as the mean ± SEM ($n = 3$, $^{**}P < 0.01$, $^{***}P < 0.001$). (**D**, **E**) p-RPA2 foci formation was increased in K1626/1628Q-reconstituted cells (arrested in G1 phase). The indicated cells were treated with IR (3 Gy) and incubated for 1 hour. HeLa cells with >10 p-RPA2 foci were counted. Over 100 cells were counted. Data are presented as the mean ± SEM ($n = 3$, $^{**}P < 0.01$, $^{***}P < 0.001$). (**F**, **G**) Rad51 foci formation was increased in K1626/1628Q-reconstituted cells. The indicated cells were treated with IR (3 Gy) and incubated for 1 hour. HeLa cells with >10 Rad51 foci were counted. Over 100 cells were counted. Data are presented as the mean ± SEM ($n = 3$, $^{**}P < 0.01$, $^{***}P < 0.001$).

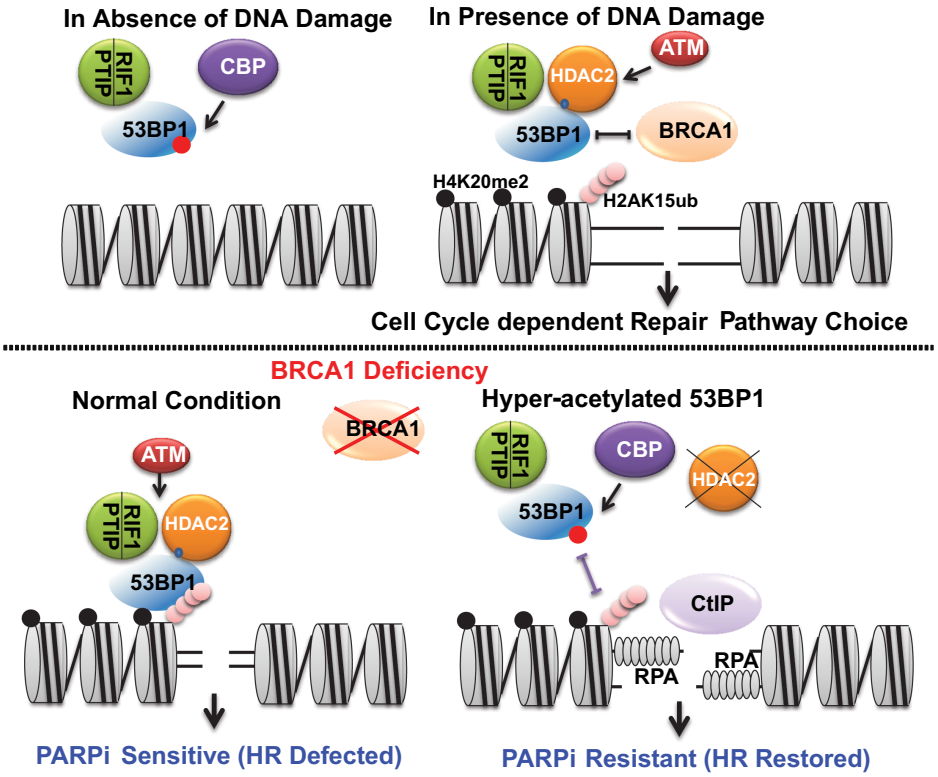

Figure 8. Working model. 53BP1 is hyperacetylated in the absence of DNA damage, and this modification is regulated by CBP. Hyperacetylated K1626/1628 prevents 53BP1 and the downstream factors PTIP and RIF1 associate with nucleosome. When DNA damage occurs, ATM-mediated phosphorylation of HDAC2 promotes the interaction of HDAC2 with 53BP1 and the deacetylation of 53BP1 at K1626/1628, which led to the association of 53BP1 with DSBs and the accumulation of 53BP1 facilitates the recruitment of PTIP, RIF1 and other NHEJ elements to damage sites. In BRCA1-deficient cells, deacetylated 53BP1 accumulates at DSBs and promotes toxic NHEJ to kill the cells in the presence of PARPi. However, hyper-acetylated 53BP1, similar as loss of 53BP1, abolishes PARPi sensitivity in BRCA1-deficient cells by restoring HR.

by CBP (Figure 3). However, acetylation is one of the most common post-translational modifications and 53BP1 is a large protein containing multiple interaction surfaces for numerous DSB-responsive proteins, so we believe it is very possible that there are other potential acetylation residues among 53BP1. For example, it would be interesting to explore that whether the acetylation of 53BP1 could affect its phosphorylation and further affect RIF1 and PTIP recruitment. We are currently improving our methodology to identify additional acetylation sites and will also investigate whether these acetylation events are important for the functions of 53BP1.

Generally, acetylation of a protein induces a conformational change and affects its interaction with other proteins or DNA by neutralizing the positive charge of the amino group (38). For example, p53 acetylation reduces its interaction with Mdm2 and SET (58,59) but increases its association with DNA (60). In our study, we reveal that the positively charged 53BP1-UDR K1626 residue interacts with the negatively charged H2A D90/E91/E92 and H2B E105 residues, while K1628 interacts with H2A E61/E64. The structure revealed that acetylation of the 53BP1-UDR K1626/1628 residues neutralizes their positive charges, thereby weakening the interaction between 53BP1-UDR and the nucleosome. 53BP1-K1626/1628Q, which mimics hyperacetylated 53BP1, showed a weaker interaction with H2A compared with WT 53BP1, indicating that the change in charge affects the conformation and nucleosome binding ability.

53BP1 must be recruited to sites of DNA damage to play a role in repair and to inhibit end resection. Previous studies on the dynamic regulation of 53BP1 recruitment to chromatin flanking DSBs focused on histone modification, such as H4K20me2 and H2AK15ub (6,37). We propose that post-translational modification of 53BP1, such as acetylation of K1626/1628 within the UDR motif, is also critical for modulating its recruitment to DNA DSBs. The UDR motif, C-terminal to the tandem Tudor domain, confers both ubiquitin and nucleosome recognition to 53BP1 and is required for the efficient formation of 53BP1 foci. In addition, Daniel Durocher's group clearly showed that the C-terminus of the UDR motif interacts with the acidic patch of H2A and is required for the interaction between 53BP1 and nucleosomes (37,38). It is consistent with our observation that CBP-mediated K1626/1628 acetylation disrupted the interaction between 53BP1 and H2A (Figure 5D and E).

53BP1 K1626/1628 acetylation is tightly regulated when DNA DSBs occur. Our data show that the 53BP1 K1626/1628 acetylation level quickly declines in response to IR and that this process is mediated by HDAC2. We found that HDAC2 is a novel substrate of ATM and that the interaction between HDAC2 and 53BP1-BRCTs is phos-

phorylation dependent. However, the DSBs recruitment of 53BP1 lacking its BRCT domains is not noticeably different from its full-length counterpart. We provide evidence that HDAC2 deacetylates 53BP1 *in vivo*, but we cannot rule out the possibility that other deacetylases in addition to HDAC2 could be able to deacetylate 53BP1. In fact, although overexpressed HDAC2 greatly reduced the acetylation level of 53BP1, overexpressed HDAC1 also reduced the 53BP1 acetylation level slightly (Figure 6A). Therefore, we believe that in addition to HDAC2, there are other HDACs or SIRTs also could deacetylate 53BP1. And the interactions between 53BP1 with other potential deacetylases may be not mediated by BRCT domain of 53BP1. Future studies are warranted to confirm whether more deacetylases are involved in regulating 53BP1 and determine the significance of 53BP1-BRCT domains on its acetylation status upon physiological and pathological cellular processes.

53BP1 K1626/1628 acetylation was enriched in S phase but limited in G1 phase (Figure 6J), while the interaction between 53BP1 and HDAC2 increased in G1 phase and decreased in S phase (Figure 6J), suggesting that 53BP1 K1626/1628 acetylation was tightly regulated by HDAC2 not only in DNA damage response but also in cell cycle stages. Future studies will be devoted to assess whether an HDAC2 pS4-derived peptide interacts directly with the 53BP1-BRCT domains and the significance of this interaction.

In this study, we revealed that the acetylation status of 53BP1 plays a key role in its recruitment to DSBs and elucidated how this specific 53BP1 modification modulates the choice of DNA repair pathway. We believe that this represents one of the ways how regulate 53BP1 accumulation at DNA break ends, not only depend on histone modification, but also is regulated by post-modification of 53BP1. Further study will focus on this acetylation dynamics and determine whether deregulation of this process contributes to broad biological significance, such as tumorigenesis and drug resistance in humans.

SUPPLEMENTARY DATA

Supplementary Data are available at NAR Online.

ACKNOWLEDGEMENTS

We are grateful Dr. Jianyuan Luo and Dr. Wenhui Zhao for the HAT expression vectors. We appreciate Dr Junjie Chen for the scientific discussion and critical reading of the manuscript. We would like to thank Yanyan Zhong, Rui Geng and Xiao Albert Zhou etc. in Wang's laboratory for insightful discussion and technical assistance.

FUNDING

National Key R&D Program of China [2017YFA0503900 and 2016YFC1302100]; National Natural Science Foundation of China [81472906 and 81672981]; Peking University [BMU20140367]; Young Talent 1000 Project [QNQR201602]. Funding for open access charge: National Natural Science Foundation of China.
Conflict of interest statement. None declared.

REFERENCES

1. Jackson,S.P. and Durocher,D. (2013) Regulation of DNA damage responses by ubiquitin and SUMO. *Mol. Cell*, **49**, 795–807.
2. Lukas,J., Lukas,C. and Bartek,J. (2011) More than just a focus: The chromatin response to DNA damage and its role in genome integrity maintenance. *Nat. Cell Biol.*, **13**, 1161–1169.
3. Panier,S. and Durocher,D. (2013) Push back to respond better: regulatory inhibition of the DNA double-strand break response. *Nat. Rev. Mol. Cell Biol.*, **14**, 661–672.
4. Chapman,J.R., Taylor,M.R. and Boulton,S.J. (2012) Playing the end game: DNA double-strand break repair pathway choice. *Mol. Cell*, **47**, 497–510.
5. Panier,S. and Boulton,S.J. (2014) Double-strand break repair: 53BP1 comes into focus. *Nat. Rev. Mol. Cell Biol.*, **15**, 7–18.
6. Zimmermann,M. and de Lange,T. (2014) 53BP1: pro choice in DNA repair. *Trends Cell Biol.*, **24**, 108–117.
7. Bryant,H.E., Schultz,N., Thomas,H.D., Parker,K.M., Flower,D., Lopez,E., Kyle,S., Meuth,M., Curtin,N.J. and Helleday,T. (2005) Specific killing of BRCA2-deficient tumours with inhibitors of poly(ADP-ribose) polymerase. *Nature*, **434**, 913–917.
8. Bunting,S.F., Callen,E., Wong,N., Chen,H.T., Polato,F., Gunn,A., Bothmer,A., Feldhahn,N., Fernandez-Capetillo,O., Cao,L. *et al.* (2010) 53BP1 inhibits homologous recombination in Brca1-deficient cells by blocking resection of DNA breaks. *Cell*, **141**, 243–254.
9. Farmer,H., McCabe,N., Lord,C.J., Tutt,A.N., Johnson,D.A., Richardson,T.B., Santarosa,M., Dillon,K.J., Hickson,I., Knights,C. *et al.* (2005) Targeting the DNA repair defect in BRCA mutant cells as a therapeutic strategy. *Nature*, **434**, 917–921.
10. Bouwman,P., Aly,A., Escandell,J.M., Pieterse,M., Bartkova,J., van der Gulden,H., Hiddingh,S., Thanasoula,M., Kulkarni,A., Yang,Q. *et al.* (2010) 53BP1 loss rescues BRCA1 deficiency and is associated with triple-negative and BRCA-mutated breast cancers. *Nat. Struct. Mol. Biol.*, **17**, 688–695.
11. Chapman,J.R., Barral,P., Vannier,J.B., Borel,V., Steger,M., Tomas-Loba,A., Sartori,A.A., Adams,I.R., Batista,F.D. and Boulton,S.J. (2013) RIF1 is essential for 53BP1-dependent nonhomologous end joining and suppression of DNA double-strand break resection. *Mol. Cell*, **49**, 858–871.
12. Zimmermann,M., Lottersberger,F., Buonomo,S.B., Sfeir,A. and de Lange,T. (2013) 53BP1 regulates DSB repair using Rif1 to control 5′ end resection. *Science*, **339**, 700–704.
13. Di Virgilio,M., Callen,E., Yamane,A., Zhang,W., Jankovic,M., Gitlin,A.D., Feldhahn,N., Resch,W., Oliveira,T.Y., Chait,B.T. *et al.* (2013) Rif1 prevents resection of DNA breaks and promotes immunoglobulin class switching. *Science*, **339**, 711–715.
14. Escribano-Diaz,C. and Durocher,D. (2013) DNA repair pathway choice–a PTIP of the hat to 53BP1. *EMBO Rep.*, **14**, 665–666.
15. Escribano-Diaz,C., Orthwein,A., Fradet-Turcotte,A., Xing,M., Young,J.T., Tkac,J., Cook,M.A., Rosebrock,A.P., Munro,M., Canny,M.D. *et al.* (2013) A cell cycle-dependent regulatory circuit composed of 53BP1-RIF1 and BRCA1-CtIP controls DNA repair pathway choice. *Mol. Cell*, **49**, 872–883.
16. Feng,L., Fong,K.W., Wang,J., Wang,W. and Chen,J. (2013) RIF1 counteracts BRCA1-mediated end resection during DNA repair. *J. Biol. Chem.*, **288**, 11135–11143.
17. Callen,E., Di Virgilio,M., Kruhlak,M.J., Nieto-Soler,M., Wong,N., Chen,H.T., Faryabi,R.B., Polato,F., Santos,M., Starnes,L.M. *et al.* (2013) 53BP1 mediates productive and mutagenic DNA repair through distinct phosphoprotein interactions. *Cell*, **153**, 1266–1280.
18. Huen,M.S., Huang,J., Leung,J.W., Sy,S.M., Leung,K.M., Ching,Y.P., Tsao,S.W. and Chen,J. (2010) Regulation of chromatin architecture by the PWWP domain-containing DNA damage-responsive factor EXPAND1/MUM1. *Mol. Cell*, **37**, 854–864.
19. Sy,S.M., Chen,J. and Huen,M.S. (2010) The 53BP1-EXPAND1 connection in chromatin structure regulation. *Nucleus*, **1**, 472–474.
20. Jacquet,K., Fradet-Turcotte,A., Avvakumov,N., Lambert,J.P., Roques,C., Pandita,R.K., Paquet,E., Herst,P., Gingras,A.C., Pandita,T.K. *et al.* (2016) The TIP60 complex regulates bivalent chromatin recognition by 53BP1 through direct H4K20me binding and H2AK15 acetylation. *Mol. Cell*, **62**, 409–421.
21. Renaud,E., Barascu,A. and Rosselli,F. (2016) Impaired TIP60-mediated H4K16 acetylation accounts for the aberrant

chromatin accumulation of 53BP1 and RAP80 in Fanconi anemia pathway-deficient cells. *Nucleic Acids Res.*, **44**, 648–656.
22. Sun,Y., Jiang,X., Chen,S., Fernandes,N. and Price,B.D. (2005) A role for the Tip60 histone acetyltransferase in the acetylation and activation of ATM. *Proc. Natl. Acad. Sci. U.S.A.*, **102**, 13182–13187.
23. Tang,J., Cho,N.W., Cui,G., Manion,E.M., Shanbhag,N.M., Botuyan,M.V., Mer,G. and Greenberg,R.A. (2013) Acetylation limits 53BP1 association with damaged chromatin to promote homologous recombination. *Nat. Struct. Mol. Biol.*, **20**, 317–325.
24. Huen,M.S., Grant,R., Manke,I., Minn,K., Yu,X., Yaffe,M.B. and Chen,J. (2007) RNF8 transduces the DNA-damage signal via histone ubiquitylation and checkpoint protein assembly. *Cell*, **131**, 901–914.
25. Kolas,N.K., Chapman,J.R., Nakada,S., Ylanko,J., Chahwan,R., Sweeney,F.D., Panier,S., Mendez,M., Wildenhain,J., Thomson,T.M. *et al.* (2007) Orchestration of the DNA-damage response by the RNF8 ubiquitin ligase. *Science*, **318**, 1637–1640.
26. Mailand,N., Bekker-Jensen,S., Faustrup,H., Melander,F., Bartek,J., Lukas,C. and Lukas,J. (2007) RNF8 ubiquitylates histones at DNA double-strand breaks and promotes assembly of repair proteins. *Cell*, **131**, 887–900.
27. An,L., Jiang,Y., Ng,H.H., Man,E.P., Chen,J., Khoo,U.S., Gong,Q. and Huen,M.S. (2017) Dual-utility NLS drives RNF169-dependent DNA damage responses. *Proc. Natl. Acad. Sci. U.S.A.*, **114**, E2872–E2881.
28. Chen,J., Feng,W., Jiang,J., Deng,Y. and Huen,M.S. (2012) Ring finger protein RNF169 antagonizes the ubiquitin-dependent signaling cascade at sites of DNA damage. *J. Biol. Chem.*, **287**, 27715–27722.
29. Kitevski-LeBlanc,J., Fradet-Turcotte,A., Kukic,P., Wilson,M.D., Portella,G., Yuwen,T., Panier,S., Duan,S., Canny,M.D., van Ingen,H. *et al.* (2017) The RNF168 paralog RNF169 defines a new class of ubiquitylated histone reader involved in the response to DNA damage. *eLife*, **6**, e23872.
30. Poulsen,M., Lukas,C., Lukas,J., Bekker-Jensen,S. and Mailand,N. (2012) Human RNF169 is a negative regulator of the ubiquitin-dependent response to DNA double-strand breaks. *J. Cell Biol.*, **197**, 189–199.
31. Mallette,F.A., Mattiroli,F., Cui,G., Young,L.C., Hendzel,M.J., Mer,G., Sixma,T.K. and Richard,S. (2012) RNF8- and RNF168-dependent degradation of KDM4A/JMJD2A triggers 53BP1 recruitment to DNA damage sites. *EMBO J.*, **31**, 1865–1878.
32. Acs,K., Luijsterburg,M.S., Ackermann,L., Salomons,F.A., Hoppe,T. and Dantuma,N.P. (2011) The AAA-ATPase VCP/p97 promotes 53BP1 recruitment by removing L3MBTL1 from DNA double-strand breaks. *Nat. Struct. Mol. Biol.*, **18**, 1345–1350.
33. Min,J., Allali-Hassani,A., Nady,N., Qi,C., Ouyang,H., Liu,Y., MacKenzie,F., Vedadi,M. and Arrowsmith,C.H. (2007) L3MBTL1 recognition of mono- and dimethylated histones. *Nat. Struct. Mol. Biol.*, **14**, 1229–1230.
34. Drane,P., Brault,M.E., Cui,G., Meghani,K., Chaubey,S., Detappe,A., Parnandi,N., He,Y., Zheng,X.F., Botuyan,M.V. *et al.* (2017) TIRR regulates 53BP1 by masking its histone methyl-lysine binding function. *Nature*, **543**, 211–216.
35. Zhang,A., Peng,B., Huang,P., Chen,J. and Gong,Z. (2017) The p53-binding protein 1-Tudor-interacting repair regulator complex participates in the DNA damage response. *J. Biol. Chem.*, **292**, 6461–6467.
36. Hu,Q., Botuyan,M.V., Cui,G., Zhao,D. and Mer,G. (2017) Mechanisms of ubiquitin-nucleosome recognition and regulation of 53BP1 chromatin recruitment by RNF168/169 and RAD18. *Mol. Cell*, **66**, 473–487.
37. Fradet-Turcotte,A., Canny,M.D., Escribano-Diaz,C., Orthwein,A., Leung,C.C., Huang,H., Landry,M.C., Kitevski-LeBlanc,J., Noordermeer,S.M., Sicheri,F. *et al.* (2013) 53BP1 is a reader of the DNA-damage-induced H2A Lys 15 ubiquitin mark. *Nature*, **499**, 50–54.
38. Wilson,M.D., Benlekbir,S., Fradet-Turcotte,A., Sherker,A., Julien,J.P., McEwan,A., Noordermeer,S.M., Sicheri,F., Rubinstein,J.L. and Durocher,D. (2016) The structural basis of modified nucleosome recognition by 53BP1. *Nature*, **536**, 100–103.
39. Sale,J.E. (2015) REV7/MAD2L2: the multitasking maestro emerges as a barrier to recombination. *EMBO J.*, **34**, 1609–1611.
40. Wang,J., Aroumougame,A., Lobrich,M., Li,Y., Chen,D., Chen,J. and Gong,Z. (2014) PTIP associates with Artemis to dictate DNA repair pathway choice. *Genes Dev.*, **28**, 2693–2698.
41. Xu,G., Chapman,J.R., Brandsma,I., Yuan,J., Mistrik,M., Bouwman,P., Bartkova,J., Gogola,E., Warmerdam,D., Barazas,M. *et al.* (2015) REV7 counteracts DNA double-strand break resection and affects PARP inhibition. *Nature*, **521**, 541–544.
42. Li,M. and Yu,X. (2015) The role of poly(ADP-ribosyl)ation in DNA damage response and cancer chemotherapy. *Oncogene*, **34**, 3349–3356.
43. Zhao,Y., Brickner,J.R., Majid,M.C. and Mosammaparast,N. (2014) Crosstalk between ubiquitin and other post-translational modifications on chromatin during double-strand break repair. *Trends Cell Biol.*, **24**, 426–434.
44. Lee,D.H., Acharya,S.S., Kwon,M., Drane,P., Guan,Y., Adelmant,G., Kalev,P., Shah,J., Pellman,D., Marto,J.A. *et al.* (2014) Dephosphorylation enables the recruitment of 53BP1 to double-strand DNA breaks. *Mol. Cell*, **54**, 512–525.
45. Orthwein,A., Fradet-Turcotte,A., Noordermeer,S.M., Canny,M.D., Brun,C.M., Strecker,J., Escribano-Diaz,C. and Durocher,D. (2014) Mitosis inhibits DNA double-strand break repair to guard against telomere fusions. *Science*, **344**, 189–193.
46. Bohgaki,M., Bohgaki,T., El Ghamrasni,S., Srikumar,T., Maire,G., Panier,S., Fradet-Turcotte,A., Stewart,G.S., Raught,B., Hakem,A. *et al.* (2013) RNF168 ubiquitylates 53BP1 and controls its response to DNA double-strand breaks. *Proc. Natl. Acad. Sci. U.S.A.*, **110**, 20982–20987.
47. Han,X., Zhang,L., Chung,J., Mayca Pozo,F., Tran,A., Seachrist,D.D., Jacobberger,J.W., Keri,R.A., Gilmore,H. and Zhang,Y. (2014) UbcH7 regulates 53BP1 stability and DSB repair. *Proc. Natl. Acad. Sci. U.S.A.*, **111**, 17456–17461.
48. Luo,J., Nikolaev,A.Y., Imai,S., Chen,D., Su,F., Shiloh,A., Guarente,L. and Gu,W. (2001) Negative control of p53 by Sir2alpha promotes cell survival under stress. *Cell*, **107**, 137–148.
49. Galanty,Y., Belotserkovskaya,R., Coates,J., Polo,S., Miller,K.M. and Jackson,S.P. (2009) Mammalian SUMO E3-ligases PIAS1 and PIAS4 promote responses to DNA double-strand breaks. *Nature*, **462**, 935–939.
50. Fukuda,T., Wu,W., Okada,M., Maeda,I., Kojima,Y., Hayami,R., Miyoshi,Y., Tsugawa,K. and Ohta,T. (2015) Class I histone deacetylase inhibitors inhibit the retention of BRCA1 and 53BP1 at the site of DNA damage. *Cancer Sci.*, **106**, 1050–1056.
51. Rodriguez,Y., Hinz,J.M. and Smerdon,M.J. (2015) Accessing DNA damage in chromatin: preparing the chromatin landscape for base excision repair. *DNA Repair*, **32**, 113–119.
52. Stengel,K.R. and Hiebert,S.W. (2015) Class I HDACs affect DNA replication, repair, and chromatin structure: implications for cancer therapy. *Antioxid. Redox Signal.*, **23**, 51–65.
53. Kaidi,A., Weinert,B.T., Choudhary,C. and Jackson,S.P. (2010) Human SIRT6 promotes DNA end resection through CtIP deacetylation. *Science*, **329**, 1348–1353.
54. Li,X., Corsa,C.A., Pan,P.W., Wu,L., Ferguson,D., Yu,X., Min,J. and Dou,Y. (2010) MOF and H4 K16 acetylation play important roles in DNA damage repair by modulating recruitment of DNA damage repair protein Mdc1. *Mol. Cell. Biol.*, **30**, 5335–5347.
55. Liu,T., Lin,Y.H., Leng,W., Jung,S.Y., Zhang,H., Deng,M., Evans,D., Li,Y., Luo,K., Qin,B. *et al.* (2014) A divergent role of the SIRT1-TopBP1 axis in regulating metabolic checkpoint and DNA damage checkpoint. *Mol. Cell*, **56**, 681–695.
56. Yuan,Z. and Seto,E. (2007) A functional link between SIRT1 deacetylase and NBS1 in DNA damage response. *Cell Cycle*, **6**, 2869–2871.
57. Dyson,H.J. and Wright,P.E. (2016) Role of intrinsic protein disorder in the function and interactions of the transcriptional coactivators CREB-binding protein (CBP) and p300. *J. Biol. Chem.*, **291**, 6714–6722.
58. Li,M., Luo,J., Brooks,C.L. and Gu,W. (2002) Acetylation of p53 inhibits its ubiquitination by Mdm2. *J. Biol. Chem.*, **277**, 50607–50611.
59. Wang,D., Kon,N., Lasso,G., Jiang,L., Leng,W., Zhu,W.G., Qin,J., Honig,B. and Gu,W. (2016) Acetylation-regulated interaction between p53 and SET reveals a widespread regulatory mode. *Nature*, **538**, 118–122.
60. Luo,J., Li,M., Tang,Y., Laszkowska,M., Roeder,R.G. and Gu,W. (2004) Acetylation of p53 augments its site-specific DNA binding both in vitro and in vivo. *Proc. Natl. Acad. Sci. U.S.A.*, **101**, 2259–2264.